

# Quality assessment of non-mydriatric fundus photographs for glaucoma screening in primary healthcare centres: a real-world study

Qi Chen ,<sup>1,2</sup> Mengtian Zhou,<sup>1</sup> Yang Cao,<sup>1</sup> Xuanli Zheng,<sup>1</sup> Huiyan Mao,<sup>1</sup> Changrong Lei,<sup>1</sup> Wanglong Lin,<sup>1</sup> Junhong Jiang,<sup>3</sup> Yize Chen,<sup>4</sup> Di Song,<sup>5</sup> Xiang Xu,<sup>1</sup> Cong Ye,<sup>1</sup> Yuanbo Liang<sup>1,6</sup>

**To cite:** Chen Q, Zhou M, Cao Y, *et al.* Quality assessment of non-mydriatric fundus photographs for glaucoma screening in primary healthcare centres: a real-world study. *BMJ Open Ophthalmology* 2023;**8**:e001493. doi:10.1136/bmjophth-2023-001493

► Additional supplemental material is published online only. To view, please visit the journal online (<http://dx.doi.org/10.1136/bmjophth-2023-001493>).

Received 13 September 2023  
Accepted 22 November 2023



© Author(s) (or their employer(s)) 2023. Re-use permitted under CC BY-NC. No commercial re-use. See rights and permissions. Published by BMJ.

For numbered affiliations see end of article.

## Correspondence to

Dr Yuanbo Liang; [yuanboliang@wmu.edu.cn](mailto:yuanboliang@wmu.edu.cn)

## ABSTRACT

**Background** This study assessed the quality distribution of non-mydriatric fundus photographs (NMFPs) in real-world glaucoma screening and analysed its influencing factors.

**Methods** This cross-sectional study was conducted in primary healthcare centres in the Yinzhou District, China, from 17 March to 3 December 2021. The quality distribution of bilateral NMFPs was assessed by the Digital Reading Department of the Eye Hospital of Wenzhou Medical University. Generalised estimating equations and logistic regression models identified factors affecting image quality.

**Results** A total of 17 232 photographs of 8616 subjects were assessed. Of these, 11.9% of images were reliable for the right eyes, while only 4.6% were reliable for the left eyes; 93.6% of images were readable in the right eyes, while 90.3% were readable in the left eyes. In adjusted models, older age was associated with decreased odds of image readability (adjusted OR (aOR)=1.07, 95% CI 1.06~1.08,  $p<0.001$ ). A larger absolute value of spherical equivalent significantly decreased the odds of image readability (all  $p<0.001$ ). Media opacity and worse visual acuity had a significantly lower likelihood of achieving readable NMFPs (aOR=1.52, 95% CI 1.31~1.75; aOR=1.70, 95% CI 1.42~2.02, respectively, all  $p<0.001$ ). Astigmatism axes within 31°~60° and 121°~150° had lower odds of image readability (aOR=1.35, 95% CI 1.11~1.63,  $p<0.01$ ) than astigmatism axes within 180°±30°.

**Conclusions** The image readability of NMFPs in large-scale glaucoma screening for individuals 50 years and older is comparable with relevant studies, but image reliability is unsatisfactory. Addressing the associated factors may be vital when implementing ophthalmological telemedicine in underserved areas.

**Trial registration number** ChiCTR2200059277.

## INTRODUCTION

As the world's leading irreversible and age-related blinding eye disease, glaucoma is often asymptomatic in its early stages,<sup>1</sup> making population screening crucial for early detection. A systemic review estimates that

## WHAT IS ALREADY KNOWN ON THIS TOPIC

- ⇒ Artificial intelligence (AI) based on high-quality fundus images excels in eye health screening.
- ⇒ However, the presence of unreliable images may impact diagnostic outcomes and exacerbate already overwhelmed healthcare systems.

## WHAT THIS STUDY ADDS

- ⇒ In this cross-sectional study, which examined 17 232 photographs of 8616 subjects, the bilateral non-mydriatric fundus photographs (NMFPs) were found to have an image reliability rate below 12%.
- ⇒ The image reliability of single-field NMFPs in large-scale glaucoma screening for individuals 50 years and older is unsatisfactory.

## HOW THIS STUDY MIGHT AFFECT RESEARCH, PRACTICE OR POLICY

- ⇒ These findings suggest that the applicability of AI based on fundus photographs for community screening in real-world settings may confront potential challenges.
- ⇒ Despite the revolutionary impact of AI-based systems in healthcare, these challenges cannot be ignored.

the number of patients with glaucoma worldwide will increase to 111.8 million in 2040.<sup>2</sup> Along with an ageing population, improved life expectancy, changing environments and behavioural patterns, healthcare systems are facing unprecedented challenges in meeting the current and anticipated demands for eye care. Although population-based screening of angle-closure glaucoma and open-angle glaucoma has been shown to be cost-effective in China,<sup>3</sup> it is still not a routine screening programme owing to ophthalmic personnel shortages and financial constraints. Encouragingly, telemedicine and artificial intelligence (AI) algorithms have revolutionised the field of eye health screening. Telemedicine enables ophthalmologists to evaluate and deliver care

remotely, which facilitates a more efficient and equitable distribution of limited healthcare resources.<sup>4–6</sup> AI-assisted screening using colour fundus photographs (CFPs) has demonstrated high sensitivity and specificity.<sup>7–12</sup> Additionally, deep learning (DL) systems have made it possible to predict the onset and progression of glaucoma.<sup>11 12</sup> Recently, Wang *et al*<sup>13</sup> developed a Markov model and concluded that annual AI telemedicine screening was the most cost-effective strategy in China.

Glaucoma screening is highly dependent on various imaging devices. Among them, fundus photography has become a valuable tool due to its high feasibility, important diagnostic value and wide availability. Obtaining high-quality CFPs is crucial for the development and application of DL systems, especially for the internal set used for training and validation.<sup>7–12</sup> However, fundus photographs acquired during real-world glaucoma screening are often non-mydratric with short shooting times and can be obscured due to media opacities such as cataracts. A certain proportion of fundus photographs obtained in population-based glaucoma screening may be deemed ‘unreadable’. Poor-quality images limit the application of AI in the healthcare industry, yet little attention has been given to the image quality of real-world fundus photographs.

In light of this, we employ a new evaluation criterion to assess the quality distribution of NMFPs obtained during real-world glaucoma screening and to analyse the factors that impact image quality. The results can serve as a valuable reference for enhancing the quality of fundus photographs in primary healthcare centres, optimising the screening approach for eye diseases and improving the efficiency of screening for those conditions.

## METHODS

This cross-sectional study was part of a randomised controlled trial (RCT) of community glaucoma screening in Yinzhou District. Informed consent was obtained from all participants. The protocol has been published on the website (<http://www.medresman.org.cn/>) with registration number ChiCTR2200059277.

### Community glaucoma screening

We randomly selected six communities to conduct glaucoma screening in Yinzhou District (Ningbo City, China). Before screening, we distributed publicity materials and propagated screening activities to community staff in advance, and community workers mobilised residents aged 50 and older to participate in the screening. Glaucoma screening was integrated with routine community health examinations in primary healthcare centres from 26 November 2020 to 3 December 2021.

### Patient and public involvement statement

Patients or the public were not involved in the design, or conduct, or reporting or dissemination plans of our research.

## Participants

Subjects included in this study were individuals aged 50 and older who underwent glaucoma screening from 17 March 2021 to 3 December 2021, and had NMFPs taken of both eyes, along with clinical diagnosis and image quality grading. Subjects who did not receive a definite image quality grade or did not complete optometry of both eyes were excluded from the study. The inclusion and exclusion diagram of the study participants is shown in online supplemental figure 1.

A total of three screening teams that underwent professional training simultaneously conducted the glaucoma screening. The screening items included registration, presenting visual acuity (PVA), intraocular pressure (IOP), automatic refractor, non-mydratric fundus photography, optical coherence tomography and handheld slit-lamp biomicroscopy. The glaucoma screening flowchart is shown in online supplemental figure 2. Ophthalmologists made diagnoses based on ophthalmic examinations and fundus reading reports. The definitions of glaucoma suspect were in accordance with the Wenzhou Glaucoma Screening Programme.<sup>14</sup> Media opacity included keratopathy, cataracts and vitreous opacity. The diagnostic criteria for cataracts included lens opacity, such as vacuoles, water clefts, lamellar separation, wheel amplitude opacity, wedge turbidity, nuclear opacity and posterior capsule opacity, but not a few punctate opacities that do not impact vision.<sup>15</sup> Additionally, a PVA of less than 0.7, except for visual impairment caused by diseases excluding cataracts, was also considered a diagnostic criterion.<sup>16</sup>

### NMFP and telemedicine reading

In the darkroom environment of primary healthcare centres, a trained operator used a digital non-mydratric fundus camera (VISUCAM 224, Zeiss, Germany) with 24 million pixels high-resolution fundus imaging to take fundus photographs of the subjects. The parameter settings of the fundus camera included the following: capture mode was colour, field of view was 45°, the flash mode was automatic flash with flash light level 5, refractive compensation range was continuous, within +35D~–35D, the working distance was 40 mm from the eye to the lens, and the internal fixation point corresponded to the midpoint of the line connecting the optic disc and the macula, which was at the centre of the photographing field. The image was meticulously focused on the posterior pole of the retina at 45°, and the photographic sequence was the right eye first, followed by the left. The operator selected and uploaded the optimal image for each eye onto the Eye Health Comprehensive Data Cloud Management Platform. Reading staff in the Digital Reading Department of the Eye Hospital of Wenzhou Medical University logged into the management platform and reviewed the image data during the screening period. The image quality was graded, the diagnosis was established by the reading staff and feedback was provided in a timely manner. The Kappa values

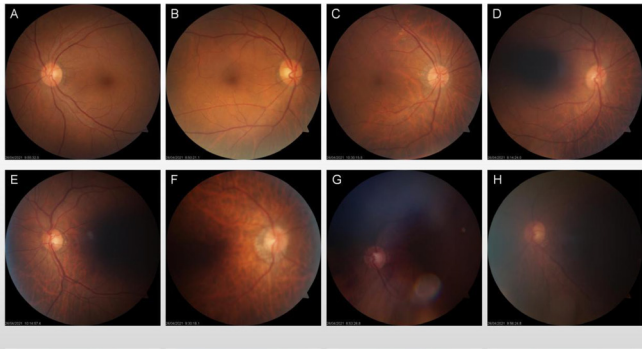


**Figure 1** Quality grading criterion for non-mydriatic fundus photographs. (A) Reliability fundus photographs. (B) Readable (both optic disc and macula visible): the photograph was mild defocus, but the results could still be interpreted. (C) Readable (both optic disc and macula visible): artefacts were discernible that did not affect the reading results. (D) Readable (optic disc only visible): the photograph was slightly defocused, but the results could still be interpreted. (E) Readable (optic disc only visible): artefacts are discernible that did not affect the reading results. (F) Unreadable: the photograph was seriously defocused that made it impossible to interpret the results. (G) Unreadable: large artefacts existed that affected the reading results. (H) Unreadable: the images were under exposed, so the optic disc was not visible.

of intraobserver agreement between image readers were 0.95~0.99, and interobserver agreement was 0.53~0.68.

### Quality grading for fundus photographs

This study established a criterion for grading fundus images to facilitate rapid population screening of glaucoma, which is mainly based on the photographic location and clarity. If the optic disc was not fully located or clearly reviewed by the reading staff, the image quality was considered unreadable. If the optic disc was clearly visible but the macular area and blood vessels were blurry, the image quality was considered readable with only the optic disc visible. If the optic disc and macular area were clearly visible but flaws such as artefacts or defocus existed, the image quality was considered readable with both the optic disc and the macula visible. If the optic disc, macular area and blood vessels were clearly visualised without obvious flaws, the image quality was considered reliable. Therefore, the image quality was divided into four levels, and details are shown as follows:

The image quality was deemed reliable according to the established criterion<sup>17</sup>: the photographs were free from defocus, blurs, underexposure or overexposure, and both the macula and the optic disc were visible and clear, as demonstrated in figure 1A.

The image quality was considered readable with both the optic disc and the macula visible. Although there was mild defocus in the photographs (as shown in figure 1B), the results could still be interpreted. Furthermore, the photographs contained easily discernible artefacts (figure 1C) that did not affect the reading results. Both

the macula and the optic disc were visible in the photographs.

The image quality was considered readable with only the optic disc visible. Although the photographs were slightly defocused (as shown in figure 1D), the results could still be interpreted. There were easily recognisable artefacts (figure 1E) that did not affect the reading results. Only the optic disc and its supratemporal and infratemporal regions were visible in the fundus photographs.

The image quality was deemed unreadable in photographs that were seriously defocused (figure 1F) and contained large artefacts that made it impossible to interpret the results (figure 1G). The images were also underexposed, and the optic disc was not visible (figure 1H).

Among them, readability included images that were readable with only the optic disc visible, images that were readable with both the optic disc and the macula visible, and reliable images. Unreadability merely included unreadable images. Reliability included reliable images. Unreliability included unreadable images, images that were readable with only the optic disc visible, and images that were readable with both the optic disc and the macula visible.

### Statistical analysis

The sample size was calculated based on a cluster RCT design. According to the annual health examination population, the gross domestic product per capita in the community and the linear distance between each community and the Eye Centre of Yinzhou People's Hospital (provided by Center for Disease Control and Prevention of Yinzhou District and Yinzhou People's Hospital), 12 selected communities were included in this study, each as a cluster. The cluster size is approximately 7000. Six control clusters and two intervention clusters would have 90% power at a 5% level of significance at two-sided to detect a difference of 39.4%<sup>18</sup> in the diagnosis rate from the intervention group compared with the control group within 1 year after screening started. Therefore, the minimum sample size was 14 000 for the screening community.

The mean±SD was used to describe normally distributed continuous variables, while the median (IQR) was used for skewed distribution data. Paired samples t-test, non-parameter test and  $\chi^2$  tests were used to compare baseline characteristics and the quality distribution of fundus photographs between both eyes. We used generalised estimating equations and logistic regression models to analyse factors affecting the image quality of both eyes. Before logistic regression analysis, we checked for collinearity among independent variables<sup>19</sup> and handled missing data on PVA and IOP through multiple imputed linear regression models.<sup>20</sup> We calculated ORs and 95% CIs to determine the risks associated with image quality. Statistical analysis was performed using SPSS V.24.0, with a significance level set at  $p < 0.05$ .



**Table 1** Baseline characteristics of the subjects included in the study

Items	OD	OS	P value
Number of eyes	8616	8616	
Age, years (median and IQR)	68 (64~73)		
Gender (male)	3545 (41.4%)		
Presenting visual acuity (logMAR)	0.22 (0.10~0.40)	0.22 (0.10~0.40)	0.654
Missing data	318 (3.7%)	319 (3.7%)	
SE, D (median and IQR)	+0.50 (-0.38~+1.13)	+0.50 (-0.38~+1.13)	0.743
≤-6D	179 (2.1%)	176 (2.0%)	
-6D~≤-3D	301 (3.5%)	281 (3.3%)	
-3D~≤0.5D	1521 (17.7%)	1499 (17.4%)	
-0.5D~0.5D	2621 (30.4%)	2659 (30.9%)	
≥0.5D	3994 (46.4%)	4001 (46.4%)	
IOP, mm Hg (median and IQR)	12.9 (10.9, 15.0)	13.3 (11.2, 15.5)	<b>&lt;0.001</b>
Missing data	182 (2.1%)	192 (2.2%)	
Diagnosed with media opacity			<b>&lt;0.001</b>
No	3286 (38.1%)	3053 (35.4%)	
Yes	5330 (61.9%)	5563 (64.6%)	
Astigmatism axis, degree (median and IQR)	94 (72, 126)	90 (73, 146)	<b>&lt;0.001</b>
1~30	980 (11.4%)	1461 (17.0%)	
31~60	533 (6.2%)	430 (5.0%)	
61~90	2829 (32.8%)	1936 (22.5%)	
91~120	1699 (19.7%)	2496 (29.0%)	
121~150	517 (6.0%)	570 (6.6%)	
151~180	2058 (23.9%)	1823 (20.0%)	

Factors with statistical significance are shown in bold.  
IOP, intraocular pressure; logMAR, logarithm of the minimum angle of resolution; OD, oculus dexter; OS, oculus sinister; SE, spherical equivalent.

## RESULTS

In total, 17 232 images from 8616 subjects (3545 male and 5071 female) were analysed (table 1). The median age of the subjects was 68 years (IQR 64~73 years). The median logMAR PVA of both eyes was 0.22 (IQR 0.10~0.40), and the spherical equivalent (SE) of both eyes was +0.5 diopters (D) (IQR -0.38~+1.13D). The median IOPs of the right and left eyes were 12.9 mm Hg (IQR 10.9~15.0 mm Hg) and 13.3 mm Hg (IQR 11.2~15.5 mm Hg), respectively. The IOP difference between bilateral eyes was statistically significant ( $p<0.001$ ). Media opacity was observed in 5330 (61.9%) right eyes and 5563 (64.6%) left eyes, and the difference was statistically significant ( $p<0.001$ ). The difference in the astigmatism axis between bilateral eyes was also statistically significant ( $p<0.001$ ).

### Quality distribution of fundus photographs between bilateral eyes

The distribution of image quality between bilateral eyes significantly differed ( $\chi^2=1968.302$ ,  $p<0.001$ ). For the right eye, 11.9% of images were reliable, 37.7% were readable with both the macula and the optic disc visible, 44% were readable with only the optic disc visible, and

6.4% were unreadable. For the left eye, 4.6% of images were reliable, 13.1% were readable with both the macula and the optic disc visible, 72.6% were readable with only the optic disc visible and 9.7% were unreadable. The bilateral image distributions of readability and reliability were also significantly different ( $\chi^2=63.925$  and  $301.134$ , respectively, all  $p<0.001$ ) (table 2).

### Factors influencing the readability of NMFPs

Our analysis using unadjusted models discovered that older age, higher absolute value of SE, media opacity, poorer visual acuity (VA) and astigmatism axis not within  $180^\circ\pm 30^\circ$  were all significantly associated with a reduced likelihood of achieving image readability (all  $p$  values  $<0.001$ ). After adjusting for age, absolute value of SE, media opacity, VA and axis orientation, we observed a significant association between older age and decreased odds of image readability (aOR=1.07, 95% CI 1.06~1.08,  $p<0.001$ ). Subjects with a larger absolute value of SE had significantly lower odds of image readability (all  $p<0.001$ ). Participants diagnosed with media opacity also showed significantly decreased odds of image readability (aOR=1.52, 95% CI 1.31~1.75,  $p<0.001$ ).

**Table 2** Quality distribution of binocular fundus photographs

Quality classification	OD	OS	Pearson $\chi^2$	P value
Unreadable	553 (6.4%)	839 (9.7%)	1968.302	<b>&lt;0.001</b>
Readable (optic disc only visible)	3789 (44.0%)	6252 (72.6%)		
Readable (both optic disc and macula visible)	3246 (37.7%)	1125 (13.1%)		
Qualified (reliability)	1028 (11.9%)	400 (4.6%)		
Unreadable	553 (6.4%)	839 (9.7%)	63.925	<b>&lt;0.001</b>
Readable	8063 (93.6%)	7777 (90.3%)		
Unreliable	7588 (88.1%)	8216 (95.4%)	301.134	<b>&lt;0.001</b>
Reliable	1028 (11.9%)	400 (4.6%)		

Factors with statistical significance are shown in bold.  
OD, oculus dexter; OS, oculus sinister.

Individuals with poorer VA had a significantly lower likelihood of achieving image readability (aOR=1.70, 95% CI 1.42~2.02,  $p<0.001$ ). Moreover, astigmatism axes within  $31^\circ\sim 60^\circ$  and  $121^\circ\sim 150^\circ$  were associated with decreased odds of image readability (aOR=1.35, 95% CI 1.11~1.63,  $p<0.01$ ) compared with astigmatism axes within  $180^\circ\pm 30^\circ$  (table 3).

#### Factors influencing the reliability of NMFPs

In univariate logistic regression models, older age, male sex, higher absolute value of SE, worse VA and smaller IOP were all associated with reduced odds of image reliability (all  $p<0.05$ ). An astigmatism axis within  $90^\circ\pm 30^\circ$  was associated with increased odds of image reliability

(OR=0.76, 95% CI 0.67~0.87,  $p<0.001$ ) compared with an astigmatism axis within  $180^\circ\pm 30^\circ$ . After adjusting for age, sex, absolute value of SE, media opacity, VA, IOP and axis orientation, a significant correlation was identified between older age and decreased odds of image reliability (aOR=1.06, 95% CI 1.05~1.07,  $p<0.001$ ). Individuals with an absolute value of SE greater than 6.0D exhibited significantly lower odds of image reliability compared with those with an absolute value of  $\leq 3.0$ D (aOR=1.98, 95% CI 1.04~3.75,  $p<0.05$ ). An astigmatism axis within  $90^\circ\pm 30^\circ$  was associated with increased odds of image reliability (OR=0.71, 95% CI 0.62~0.81,  $p<0.001$ ) compared with an astigmatism axis within  $180^\circ\pm 30^\circ$  (table 4).

**Table 3** Logistics regression of factors affecting image readability

	Unadjusted OR	P value*	Adjusted OR	P value†
Age (years)	1.08 (1.07~1.09)	<b>&lt;0.001</b>	1.07 (1.06~1.08)	<b>&lt;0.001</b>
Gender				
Male	1 (ref.)			
Female	1.00 (0.88~1.13)	0.950		
Absolute value of SE (D)				
$\leq 3.0$	1 (ref.)		1 (ref.)	
$>3.0$ and $\leq 6.0$	2.40 (1.93~3.00)	<b>&lt;0.001</b>	2.49 (1.75~3.55)	<b>&lt;0.001</b>
$> 6.0$	2.91 (2.14~3.97)	<b>&lt;0.001</b>	1.69 (1.33~2.14)	<b>&lt;0.001</b>
Diagnosed with media opacity				
No	1 (ref.)		1 (ref.)	
Yes	1.71 (1.49~1.97)	<b>&lt;0.001</b>	1.52 (1.31~1.75)	<b>&lt;0.001</b>
Visual acuity (logMAR)	2.63 (2.23~3.09)	<b>&lt;0.001</b>	1.70 (1.42~2.02)	<b>&lt;0.001</b>
IOP (mm Hg)	0.99 (0.97~1.01)	0.184		
Axis orientation (degree)				
1~30 and 151~180	1 (ref.)		1 (ref.)	
31~60 and 121~150	1.46 (1.22~1.76)	<b>&lt;0.001</b>	1.35 (1.11~1.63)	<b>0.003</b>
61~90 and 91~120	1.27 (1.12~1.45)	<b>&lt;0.001</b>	1.09 (0.95~1.25)	0.223

\*Univariate logistic regression models without adjusted variables.

†Multivariate logistic regression models, adjusted for age, absolute value of SE, media opacity, visual acuity and axis orientation. IOP, intraocular pressure; logMAR, logarithm of the minimum angle of resolution; SE, spherical equivalent.

**Table 4** Logistics regression of factors affecting image reliability

	Unadjusted OR	P value*	Adjusted OR	P value†
Age (years)	1.05 (1.04~1.06)	<0.001	1.06 (1.05~1.07)	<0.001
Gender				
Male	1 (ref.)		1 (ref.)	
Female	0.85 (0.75~0.97)	0.017	0.90 (0.78~1.03)	0.121
Absolute value of SE (D)				
≤3.0	1 (ref.)		1 (ref.)	
>3.0 and ≤6.0	1.43 (1.04~1.97)	0.027	1.37 (0.96~1.96)	0.080
> 6.0	1.82 (1.03~3.21)	0.038	1.98 (1.04~3.75)	0.037
Diagnosed with media opacity				
No	1 (ref.)		1 (ref.)	
Yes	1.12 (0.98~1.27)	0.092	0.88 (0.76~1.01)	0.062
Visual acuity (logMAR)	1.56 (1.17~2.09)	0.003	1.08 (0.81~1.45)	0.583
IOP (mm Hg)	0.97 (0.96~0.99)	0.001	0.99 (0.97~1.01)	0.356
Axis orientation (degree)				
1~30 and 151~180	1 (ref.)		1 (ref.)	
31~60 and 121~150	0.92 (0.75~1.11)	0.377	0.90 (0.73~1.11)	0.314
61~90 and 91~120	0.76 (0.67~0.87)	<0.001	0.71 (0.62~0.81)	<0.001

\*Univariate logistic regression models without adjusted variables.

†Multivariate logistic regression models, adjusted for age, gender, absolute value of SE, media opacity, visual acuity, IOP and axis orientation.

IOP, intraocular pressure; logMAR, logarithm of the minimum angle of resolution; SE, spherical equivalent.

## DISCUSSION

This study first reported the distribution of image quality for glaucoma screening and related influencing factors in China. The fundus images of previous studies mostly originated from the clinic and mydriatic,<sup>21 22</sup> and image quality was graded for the detection of disease-specific features. However, fundus abnormalities in large-scale glaucoma screening in communities vary widely. Because this study was conducted in the context of comprehensive eye health screening primarily focused on glaucoma, image readability was the primary concern. Accurate diagnosis of glaucoma relied on high-quality fundus photography, with particular emphasis on capturing the discrimination range of the optic disc and its surrounding two papillary diameters. This was critical for identifying the vertical cup-disc ratio, as well as the width of the superior temporal or inferior temporal disc edge and retinal nerve fibre layer.<sup>23</sup> The readability of bilateral image quality was found to be above 90%, which was a higher rate compared with previous telemedicine programmes that used NMFP.<sup>24–26</sup> This difference could be due to variations in the definition of unreadable images. Additionally, multiple age-related eye diseases tend to coexist and exacerbate each other in elderly individuals.<sup>27</sup> The primary objective of screening was to refer individuals with suspected eye diseases and prevent cases of missed diagnosis. Comprehensive eye health screening could serve as a relatively cost-effective screening model, which would help to address issues related to high screening

costs and low efficiency. As a result, it was recommended that four specific areas of a single-field fundus photograph—the optic disc, macular area and the first branch of the upper and lower retinal vascular arch—should be clearly visible as the standard for determining image reliability.<sup>28</sup> However, the reliability of bilateral image quality in our study was found to be less than 12%, which was lower than previously reported.<sup>29</sup> This indicated that the quality of real-world NMFPs fell far short of meeting this criterion. During the screening process, factors such as improper eye fixation, miosis, blepharoptosis, inaccurate focus, excessive or insufficient exposure, and lens opacity might contribute to a decline in the quality of fundus photographs. This could, in turn, distinctly impact the overall effectiveness of NMFP as a tool for population-based screening of fundus diseases in real-world settings.

Our study showed that the image readability and reliability of the right eyes were consistently better than those of the left eyes. There could be several reasons for this, including the photography sequence and insufficient inter-photograph intervals, which could lead to inadequate pupil dilation and the proportion difference of media opacity, subsequently, more unreadable or unreliable images for the left eyes. In addition, the postillumination pupil response (PIPR)<sup>30 31</sup> was sustained pupil constriction that occurred after light cessation, of which redilation velocity was its quantified metric. The PIPR redilation velocity has been found to increase with decreasing irradiance, shorter stimulus duration and longer wavelengths.<sup>32</sup> A previous

study<sup>30</sup> reported that the maximum duration of PIPR in healthy participants was 83.0±48.0s for 1s pulsed light stimulation. Lamirel *et al*<sup>28</sup> found that taking high-quality photographs with an interphotograph interval of 30–90s was 3.8 times more effective than intervals of <15s. Our glaucoma screening was integrated into the community health examination, with a maximum of nearly 130 subjects being examined in the morning. We speculated that the bilateral photography interval during onsite screening fell within the PIPR period, especially for the left eyes, which worsened the image quality. These findings were essential for community-based screening programmes that primarily relied on NMFPs. A prospective study might be conducted in the future to find a suitable photographic interval.

This study also showed that older age, media opacity and poorer VA were associated with a decreased likelihood of obtaining readable fundus images, and older age was also associated with significantly decreased odds of image reliability. These findings were consistent with previous studies based on NMFPs.<sup>24 28 29 33</sup> It was likely that older participants were more vulnerable to ocular media opacity and miosis, which could deteriorate image quality. Previous studies<sup>34–36</sup> found that unoperated cataracts were a primary cause of visual impairment and blindness. Hark *et al*<sup>24</sup> established that the rate of visually significant cataracts in participants with unreadable images was twice as high as that in readable images ( $p<0.05$ ). Therefore, the image readability of subjects with poorer VA was susceptible to media opacity.

We observed a novel finding that a higher absolute value of SE was associated with lower odds of fundus image readability and reliability. This could be attributed to poor fixation in individuals with high myopia or hyperopia, which might limit the fundus camera's ability to fully compensate for ametropia. Our findings also indicated that oblique astigmatism was associated with a lower likelihood of image readability compared with with-the-rule (WTR) astigmatism, and against-the-rule (ATR) astigmatism was associated with a significantly higher likelihood of image reliability compared with WTR astigmatism. Regular astigmatism takes three different forms,<sup>32</sup> and previous studies have shown that corneal irregular astigmatism was greatest in eyes with oblique astigmatism, even after adjustment for age in a stepwise multiple regression model. This was followed by WTR astigmatism and then ATR astigmatism.<sup>32</sup> Corneal irregular astigmatism is known to increase with age and various corneal diseases.<sup>37–39</sup> We speculated that eyes with oblique astigmatism have the largest corneal irregularity astigmatism, followed by WTR astigmatism and then ATR astigmatism, so the image readability of eyes with oblique astigmatism was worse than that of WTR astigmatism, and the image reliability of eyes with ATR astigmatism was better than that of WTR astigmatism.

There were several limitations in our study. First, due to the screening process, we were unable to collect comprehensive sociodemographic information from the participants. Second, we did not grade the severity of media opacity, particularly cataracts, which could have affected image quality. Additionally, we did not perform

dilated fundus photography, as this was not feasible in a large-scale community-based screening with a high population density. Furthermore, it should be noted that subjects with narrow angle anatomy may be at risk of acute angle-closure glaucoma attacks when their pupils are dilated. Third, to provide timely feedback regarding diagnosis during onsite screening, we did not conduct hierarchical image reading. However, the reading staff had more than 10 years of experience in retina reading, and the interobserver and intraobserver agreement was moderate to high. Finally, due to a large number of individuals usually making appointments for health examinations everyday during the screening period, we did not investigate different photographic conditions on image quality, such as photography intervals, exposure intensity and so on. Meanwhile, recently different fundus cameras such as ultra-wide fundus imaging, retro-mode imaging based on confocal scanning laser ophthalmoscopy and fundus adaptive optics scanning laser ophthalmoscope emerged rapidly. These cameras greatly improved the quality and resolution of fundus imaging compared with traditional fundus cameras, especially for old population with media opacity, and without pharmacological pupil dilation. These fundus imaging techniques might improve the image reliability in the real world.

Our study suggests that single-field NMFPs can be used for large-scale glaucoma screening in the general population over 50 years old, but the reliability of the images may be compromised. Age, absolute value of SE, media opacity and VA are significant factors that affect image quality. Oblique astigmatism is associated with worse image readability than WTR astigmatism, while ATR astigmatism is associated with better image reliability than WTR astigmatism. These findings highlight the importance of addressing these factors to improve the effectiveness of ophthalmological telemedicine and to optimise the screening mode for eye diseases in underserved areas.

#### Author affiliations

<sup>1</sup>National Clinical Research Center for Ocular Diseases, Eye Hospital, Wenzhou Medical University, Wenzhou, Zhejiang, China

<sup>2</sup>Department of Ophthalmology, The Second Affiliated Hospital of Zhengzhou University, Zhengzhou, Henan, China

<sup>3</sup>Department of Ophthalmology, Shanghai General Hospital, National Clinical Research Center for Eye Diseases, Shanghai Jiao Tong University School of Medicine, Shanghai, China

<sup>4</sup>Department of Ophthalmology, First Hospital of Shanxi Medical University, Taiyuan, China

<sup>5</sup>Department of Ophthalmology, The First People's Hospital of Huzhou, The First Affiliated Hospital of Huzhou Teacher College, Huzhou, China

<sup>6</sup>Glaucoma Research Institute, Wenzhou Medical University, Wenzhou, China

**Contributors** QC, MZ, YC, XZ, HM, CL and WL performed material preparation, data collection, or interpretation of data and takes responsibility for the integrity of the data. QC, MZ, YC, JJ, YC and DS contributed to the study conception, QC participated in literature search, data analysis, drafted and revised the manuscript. Critical revision of the manuscript for important intellectual content: all authors. Administrative, technical or material support: CY and YL. YL was responsible for the overall content as guarantor.



**Funding** This study was supported by the National Key Research and Development Project of China (No. 2020YFC2008200); the Program for Zhejiang Leading Talent of S&T Innovation (No. 2021R52012).

**Competing interests** None declared.

**Patient and public involvement** Patients and/or the public were not involved in the design, or conduct, or reporting or dissemination plans of this research.

**Patient consent for publication** Not applicable.

**Ethics approval** The Ethics Committee of the Eye Hospital of Wenzhou Medical University (Wenzhou, China) granted approval for this study prior to its commencement with reference number 2019-209-K-186, which was conducted in accordance with the principles outlined in the Declaration of Helsinki. Participants gave informed consent to participate in the study before taking part.

**Provenance and peer review** Not commissioned; externally peer reviewed.

**Data availability statement** Data are available upon reasonable request.

**Supplemental material** This content has been supplied by the author(s). It has not been vetted by BMJ Publishing Group Limited (BMJ) and may not have been peer-reviewed. Any opinions or recommendations discussed are solely those of the author(s) and are not endorsed by BMJ. BMJ disclaims all liability and responsibility arising from any reliance placed on the content. Where the content includes any translated material, BMJ does not warrant the accuracy and reliability of the translations (including but not limited to local regulations, clinical guidelines, terminology, drug names and drug dosages), and is not responsible for any error and/or omissions arising from translation and adaptation or otherwise.

**Open access** This is an open access article distributed in accordance with the Creative Commons Attribution Non Commercial (CC BY-NC 4.0) license, which permits others to distribute, remix, adapt, build upon this work non-commercially, and license their derivative works on different terms, provided the original work is properly cited, appropriate credit is given, any changes made indicated, and the use is non-commercial. See: <http://creativecommons.org/licenses/by-nc/4.0/>.

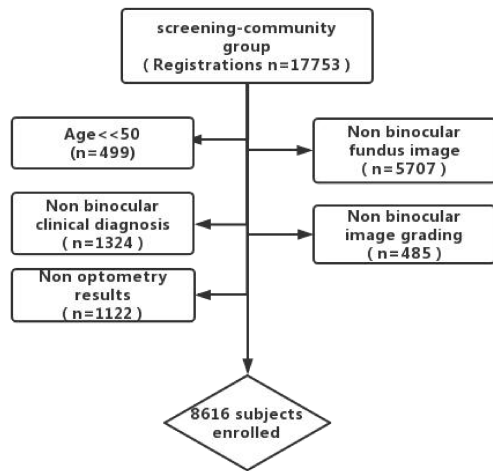
#### ORCID iD

Qi Chen <http://orcid.org/0000-0003-2546-1869>

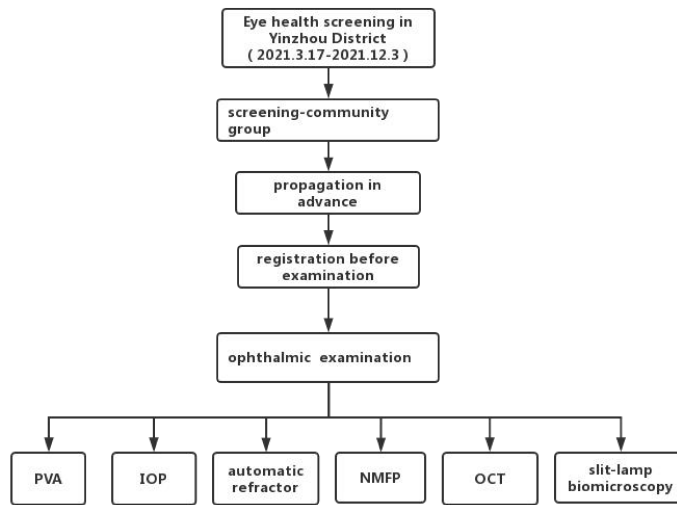
#### REFERENCES

- Heijl A, Bengtsson B, Oskarsdottir SE. Prevalence and severity of undetected manifest glaucoma: results from the early manifest glaucoma trial screening. *Ophthalmology* 2013;120:1541–5.
- Tham Y-C, Li X, Wong TY, et al. Global prevalence of glaucoma and projections of glaucoma burden through 2040: a systematic review and meta-analysis. *Ophthalmology* 2014;121:2081–90.
- Tang J, Liang Y, O'Neill C, et al. Cost-effectiveness and cost-utility of population-based glaucoma screening in China: a decision-analytic Markov model. *Lancet Glob Health* 2019;7:e968–78.
- Li J-P, Liu H, Ting DSJ, et al. Digital technology, TELE-medicine and artificial intelligence in ophthalmology: a global perspective. *Prog Retin Eye Res* 2021;82:100900.
- Wickham L, Hay G, Hamilton R, et al. The impact of COVID policies on acute ophthalmology services-experiences from Moorfields eye hospital NHS foundation trust. *Eye (Lond)* 2020;34:1189–92.
- Bourdon H, Jaillant R, Ballino A, et al. Teleconsultation in primary ophthalmic emergencies during the COVID-19 lockdown in Paris: experience with 500 patients in March and April 2020. *J Fr Ophtalmol* 2020;43:577–85.
- Liu H, Li L, Wormstone IM, et al. Development and validation of a deep learning system to detect glaucomatous optic neuropathy using fundus photographs. *JAMA Ophthalmol* 2019;137:1353–60.
- Sengupta S, Singh A, Leopold HA, et al. Ophthalmic diagnosis using deep learning with fundus images - a critical review. *Artif Intell Med* 2020;102:101758.
- Ting DSW, Pasquale LR, Peng L, et al. Artificial intelligence and deep learning in ophthalmology. *Br J Ophthalmol* 2019;103:167–75.
- Li Z, He Y, Keel S, et al. Efficacy of a deep learning system for detecting glaucomatous optic neuropathy based on color fundus photographs. *Ophthalmology* 2018;125:1199–206.
- Devalla SK, Liang Z, Pham TH, et al. Glaucoma management in the era of artificial intelligence. *Br J Ophthalmol* 2020;104:301–11.
- Li F, Su Y, Lin F, et al. A deep-learning system predicts glaucoma incidence and progression using retinal photographs. *J Clin Invest* 2022;132:e157968.
- Liu H, Li R, Zhang Y, et al. Economic evaluation of combined population-based screening for multiple blindness-causing eye diseases in China: a cost-effectiveness analysis. *Lancet Glob Health* 2023;11:e456–65.
- Liang Y, Jiang J, Ou W, et al. Effect of community screening on the demographic makeup and clinical severity of glaucoma patients receiving care in urban China. *Am J Ophthalmol* 2018;195:1–7.
- Chylack LT, Wolfe JK, Singer DM, et al. The lens opacities classification system III. The longitudinal study of cataract study group. *Arch Ophthalmol* 1993;111:831–6.
- Zhao J, Sui R, Jia L, et al. Visual acuity and quality of life outcomes in patients with cataract in Shunyi County, China. *Am J Ophthalmol* 1998;126:515–23.
- Fundus Disease Group of Ophthalmology Branch of Chinese Medical Association, Fundus Disease Professional Committee of Ophthalmologists Branch of Chinese Medical Doctor Association. Guidelines for image acquisition and film reading for diabetic retinopathy screening in China. *Chin J Ophthalmol* 2017;53:890–6.
- Grodum K, Heijl A, Bengtsson B. A comparison of glaucoma patients identified through mass screening and in routine clinical practice. *Acta Ophthalmol Scand* 2002;80:627–31.
- Khalili S, Faradmal J, Mahjub H, et al. Overcoming the problems caused by collinearity in mixed-effects logistic model: determining the contribution of various types of violence on depression in pregnant women. *BMC Med Res Methodol* 2021;21:154.
- Austin PC, White IR, Lee DS, et al. Missing data in clinical research: a tutorial on multiple imputation. *Can J Cardiol* 2021;37:1322–31.
- Kubin A-M, Wirkkala J, Kesitalo A, et al. Handheld fundus camera performance, image quality and outcomes of diabetic retinopathy grading in a pilot screening study. *Acta Ophthalmol* 2021;99:e1415–20.
- Laurik-Feuerstein KL, Sapahia R, Cabrera DeBuc D, et al. The assessment of fundus image quality labeling reliability among graders with different backgrounds. *PLoS One* 2022;17:e0271156.
- Hagiwara Y, Koh JEW, Tan JH, et al. Computer-aided diagnosis of glaucoma using fundus images: a review. *Comput Methods Programs Biomed* 2018;165:1–12.
- Hark LA, Myers JS, Rahmatnejad K, et al. Philadelphia telemedicine glaucoma detection and follow-up study: analysis of unreadable fundus images. *J Glaucoma* 2018;27:999–1008.
- Conlin PR, Asefzadeh B, Pasquale LR, et al. Accuracy of a technology-assisted eye exam in evaluation of referable diabetic retinopathy and concomitant ocular diseases. *Br J Ophthalmol* 2015;99:1622–7.
- Murgatroyd H, Ellingford A, Cox A, et al. Effect of mydriasis and different field strategies on digital image screening of diabetic eye disease. *Br J Ophthalmol* 2004;88:920–4.
- Voleti VB, Hubschman JP. Age-related eye disease. *Maturitas* 2013;75:29–33.
- Lamirel C, Bruce BB, Wright DW, et al. Quality of nonmydriatic digital fundus photography obtained by nurse practitioners in the emergency department: the FOTO-ED study. *Ophthalmology* 2012;119:617–24.
- Lin T-C, Chiang Y-H, Hsu C-L, et al. Image quality and diagnostic accuracy of a Handheld Nonmydriatic fundus camera: feasibility of a Telemedical approach in screening retinal diseases. *J Chin Med Assoc* 2020;83:962–6.
- Adhikari P, Zele AJ, Feigl B. The post-illumination pupil response (PIPR). *Invest Ophthalmol Vis Sci* 2015;56:3838–49.
- Kankipati L, Girkin CA, Gamlin PD. The post-illumination pupil response is reduced in glaucoma patients. *Invest Ophthalmol Vis Sci* 2011;52:2287–92.
- Ueno Y, Nomura R, Hiraoka T, et al. Comparison of corneal irregular astigmatism by the type of corneal regular Astigmatism. *Sci Rep* 2021;11:15769.
- Davila JR, Sengupta SS, Niziol LM, et al. Predictors of photographic quality with a Handheld Nonmydriatic fundus camera used for screening of vision-threatening diabetic retinopathy. *Ophthalmologica* 2017;238:89–99.
- Nangia V, Jonas JB, George R, et al. Prevalence and causes of blindness and vision impairment: magnitude, temporal trends and projections in South and central Asia. *Br J Ophthalmol* 2019;103:871–7.
- Xu T, Wang B, Liu H, et al. Prevalence and causes of vision loss in China from 1990 to 2019: findings from the Global Burden of Disease Study 2019. *Lancet Public Health* 2020;5:e682–91.
- Zhao J, Xu X, Ellwein LB, et al. Causes of visual impairment and blindness in the 2006 and 2014 nine-province surveys in rural China. *Am J Ophthalmol* 2019;197:80–7.
- Namba H, Sugano A, Nishi K, et al. Age-related variations in corneal geometry and their association with astigmatism: the Yamagata study (Funagata). *Medicine (Baltimore)* 2018;97:e12894.
- Namba H, Sugano A, Murakami T, et al. Age-related changes in astigmatism and potential causes. *Cornea* 2020;39 Suppl 1:S34–8.
- Shao X, Zhou K-J, Pan A-P, et al. Age-related changes in corneal astigmatism. *J Refract Surg* 2017;33:696–703.





Supplemental Figure 1. Inclusion and exclusion diagram of study participants



Supplemental Figure2. Glaucoma screening Flowchart